Mycologia

ISSN: (Print) (Online) Journal homepage: www.tandfonline.com/journals/umyc20

Fusarium xyrophilum, sp. nov., a member of the *Fusarium fujikuroi* species complex recovered from pseudoflowers on yellow-eyed grass (*Xyris* spp.) from Guyana

Imane Laraba, Hye-Seon Kim, Robert H. Proctor, Mark Busman, Kerry O'Donnell, Frederick C. Felker, M. Catherine Aime, Rachel A. Koch & Kenneth J. Wurdack

To cite this article: Imane Laraba, Hye-Seon Kim, Robert H. Proctor, Mark Busman, Kerry O'Donnell, Frederick C. Felker, M. Catherine Aime, Rachel A. Koch & Kenneth J. Wurdack (2020) *Fusarium xyrophilum*, sp. nov., a member of the *Fusarium fujikuroi* species complex recovered from pseudoflowers on yellow-eyed grass (*Xyris* spp.) from Guyana, Mycologia, 112:1, 39-51, DOI: 10.1080/00275514.2019.1668991

To link to this article: https://doi.org/10.1080/00275514.2019.1668991

MYCOLOGIA
2020, VOL. 112, NO. 1, 39–51
https://doi.org/10.1080/00275514.2019.1668991

Taylor & Francis
Taylor & Francis Group

Fusarium xyrophilum, sp. nov., a member of the *Fusarium fujikuroi* species complex recovered from pseudoflowers on yellow-eyed grass (*Xyris* spp.) from Guyana

Imane Laraba[a], Hye-Seon Kim[a], Robert H. Proctor[a], Mark Busman[a], Kerry O'Donnell[a], Frederick C. Felker[b], M. Catherine Aime[c], Rachel A. Koch[c], and Kenneth J. Wurdack[d]

[a]Mycotoxin Prevention and Applied Microbiology Research Unit, National Center for Agricultural Utilization Research, Agricultural Research Service, US Department of Agriculture, Peoria, Illinois 61604-3999; [b]Functional Food Research Unit, National Center for Agricultural Utilization Research, Agricultural Research Service, US Department of Agriculture, Peoria, Illinois 61604-3999; [c]Department of Botany and Plant Pathology, Purdue University, West Lafayette, Indiana 47907-2054; [d]Department of Botany, National Museum of Natural History, Smithsonian Institution, Washington, DC 20013-2012

ABSTRACT
We report on the discovery and characterization of a novel *Fusarium* species that produced yellow-orange pseudoflowers on *Xyris* spp. (yellow-eyed grass; Xyridaceae) growing in the savannas of the Pakaraima Mountains of western Guyana. The petaloid fungal structures produced on infected plants mimic host flowers in gross morphology. Molecular phylogenetic analyses of full-length *RPB1* (RNA polymerase largest subunit), *RPB2* (RNA polymerase second largest subunit), and *TEF1* (elongation factor 1-α) DNA sequences mined from genome sequences resolved the fungus, described herein as *F. xyrophilum*, sp. nov., as sister to *F. pseudocircinatum* within the African clade of the *F. fujikuroi* species complex. Results of a polymerase chain reaction (PCR) assay for mating type idiomorph revealed that single-conidial isolates of *F. xyrophilum* had only one of the *MAT* idiomorphs (*MAT1-1* or *MAT1-2*), which suggests that the fungus may have a heterothallic sexual reproductive mode. BLASTn searches of whole-genome sequence of three strains of *F. xyrophilum* indicated that it has the genetic potential to produce secondary metabolites, including phytohormones, pigments, and mycotoxins. However, a polyketide-derived pigment, 8-*O*-methylbostrycoidin, was the only metabolite detected in cracked maize kernel cultures. When grown on carnation leaf agar, *F. xyrophilum* is phenotypically distinct from other described *Fusarium* species in that it produces aseptate microconidia on erect indeterminate synnemata that are up to 2 mm tall and it does not produce multiseptate macroconidia.

ARTICLE HISTORY
Received 22 July 2019
Accepted 13 September 2019

KEYWORDS
Floral mimicry; *MAT* idiomorphs; molecular phylogenetics; morphology; *RPB1*; *RPB2*; synnemata; *TEF1*; whole genome; 1 new taxon

INTRODUCTION

Fusarium is widely regarded as the most important genus of mycotoxin-producing plant pathogens (Aoki et al. 2015). Fusaria and their toxins pose a global threat to agricultural biosecurity, food safety, and human health. Fusarial diseases are responsible for multibillion-dollar annual losses to US and the world's agricultural economy. Over the past two decades, intensive molecular phylogenetic analyses of *Fusarium* strains housed in the Agricultural Research Service (ARS) Culture Collection (NRRL), the *Fusarium* Research Center (FRC), and the Westerdijk Fungal Biodiversity Institute (CBS) indicate that this genus contains over 300 phylogenetically distinct species as assessed by the genealogical concordance phylogenetic species concept sensu Taylor et al. (2000). As presently circumscribed, *Fusarium* comprises 23 monophyletic species complexes and five single-species lineages (Laurence et al. 2011; O'Donnell et al. 2013; Summerell 2019).

Phytopathogenic fusaria can establish localized or systemic infections and incite economically important diseases in a plethora of agronomically, silviculturally, and horticulturally important plants (Leslie and Summerell 2006). Examples of fusaria inducing disease symptoms on various plant parts include root rot of soybean (Srivastava et al. 2014), crown rot of wheat (Laraba et al. 2018), stalk rot of corn (Santiago et al. 2010), head blight of wheat and barley (Kelly et al. 2015), and malformation of mango inflorescences (Marasas et al. 2006).

Numerous fungi can induce significant changes to inflorescences. For example, some *Fusarium* species can cause mango malformation disease, which includes proliferation of enlarged and sterile mango flowers that are unable to develop into fruit (Nicholson and Van Staden

---

CONTACT Imane Laraba imane.laraba@usda.gov
Supplemental data for this article can be accessed on the publisher's Web site.

1988; Otero-Colina et al. 2010), and some strains of *F. verticillioides* alter flower phenology of the Mexican medicinal plant *Moussonia deppeana* (Lara and Ornelas 2003). In contrast, fungi that induce flower-like structures (i.e., pseudoflowers) that mimic the visual and/or olfactory floral traits of the host appear to be exceedingly rare. Thus far, pseudoflower induction has been reported only by several rust species (Roy 1993; Pfunder and Roy 2000; Naef et al. 2002) and *Monilinia vaccinii-corymbosi*, the cause of mummy berry of blueberry and huckleberry (Batra and Batra 1985; McArt et al. 2016). Pseudoflowers that have been examined thus far attract pollinators that vector infective spores to new hosts and facilitate sexual outcrossing of the fungi that induce them (Roy 1993; Raguso and Roy 1998; Gronquist et al. 2001; Ngugi and Scherm 2006; McArt et al. 2016).

The present study was prompted by the collection of bright yellow-orange pseudoflowers on *Xyris* species (yellow-eyed grass) growing in the upland savannas of the Pakaraima Mountains in western Guyana in 2010 and 2012. In prior botanical reports of these pseudoflowers, the cause was initially suggested to be a smut fungus (Kral 1988; Kelloff 2003). To our knowledge, the etiological agent(s) has not been identified. Therefore, the objectives of the present study were to (i) identify the fungus (or fungi) in the pseudoflowers and evaluate its evolutionary relationships with other fungi by molecular phylogenetic analyses; (ii) formally describe the fungus as *Fusarium xyrophilum*, sp. nov.; (iii) evaluate the potential of *F. xyrophilum* to undergo sexual reproduction; (iv) predict its genetic potential to produce secondary metabolites based on analyses of whole-genome sequence data; and (vi) determine whether the fungus can produce secondary metabolites in culture.

MATERIALS AND METHODS

Host collections and fungal isolates.—*Xyris surinamensis* and *X. setigera* plants bearing pseudoflowers that mimic true flowers in gross morphology (FIG. 1A–C) were collected in the Cuyuni-Mazaruni Region of Guyana in Jul 2010 (KJW 5502, 5508, and 5226; TABLE 1) and May 2012 (KJW 5664 and 5665; TABLE 1). Plant material was dried in the field using a silica gel protocol (Chase and Hills 1991) and then stored at −20 C. The three collections from 2010 did not contain viable conidia. However, single-spore cultures were obtained from the dried specimens collected in 2012 (KJW 5664 and 5665; TABLE 2) by culturing microconidia from the pseudoflowers on 3% water agar amended with 2 mL/L of an antibiotic solution (P4083; 5000 units penicillin G, 5 mg streptomycin, and 10 mg neomycin per mL; Sigma-Aldrich, St. Louis, Missouri). Selected isolates were accessioned in the ARS Culture Collection (https://nrrl.ncaur.usda.gov/; TABLE 2) where they are available for distribution upon request. To characterize the internal features of the pseudoflowers on *X. surinamensis*, they were rehydrated in ultrapure water for 24 h at 25 C, dehydrated in a graded ethanol series, freeze-fractured in liquid nitrogen with a single-edge razor blade (O'Donnell and Hooper 1977), and dried in a Samdri-PVT-3D critical point dryer (Tousimis, Rockville, Maryland). For scanning electron microscopy (SEM), the dried pseudoflowers were mounted on stubs, coated with gold in a SPI sputter coater (Structure Probe, West Chester, Pennsylvania), and examined using a JEOL JSM-6010A microscope (Tokyo, Japan).

Molecular phylogenetics and whole-genome sequencing.—DNA extracted from a silica gel–dried pseudoflower collected in 2010 (KJW 5508; TABLE 1), using a cetyltrimethylammonium bromide protocol (CTAB; Sigma-Aldrich, St. Louis, Missouri; Gardes and Bruns 1993), was polymerase chain reaction (PCR)-amplified and sequenced with nuclear ribosomal internal transcribed spacer (ITS rDNA) primer pair 5 × 4 (White et al. 1990). In addition, the conserved 3′ end of translation elongation factor 1-α (*TEF1*) was PCR-amplified and sequenced using primer pair EF1-983F (5′-GCYCCYGGHCAYCGTGAYTTYAT) × EF1-2218R (5′-ATGACACCRACRGCRACRGTYTG) (Rehner and Buckley 2005) from silica gel–dried pseudoflowers collected in 2010 (KJW 5226) and 2012 (KJW 5664) (TABLE 1). In addition, isolates recovered from pseudoflowers (TABLE 2) were cultured at 25 C in yeast-malt broth (20 g glucose, 5 g peptone, 3 g yeast extract, and 3 g malt extract per 1 L water) on a rotary shaker set at 150 rpm. After incubation for 3–4 d, the resulting mycelia were harvested over a Büchner funnel, freeze-dried overnight, and total genomic DNA was extracted as described above. Phylogenetic analyses of the isolates were conducted by using Sanger sequences of PCR-amplified fragments of translation elongation factor 1-α (*TEF1*) and the genes encoding the largest (*RPB1*) and second largest (*RPB2*) subunits of RNA polymerase obtained with an ABI 3730 Genetic Analyzer (ABI, Emeryville, California) as previously described (O'Donnell et al. 2000, 2013). Resulting ABI sequence chromatograms were edited with Sequencher 5.2.4 (Gene Codes, Ann Arbor, Michigan) and aligned with MUSCLE (Edgar 2004) in SeaView 4.3.0 (Gouy et al. 2009). In addition, a ZR Fungal/Bacterial DNA MiniPrep kit (Zymo Research, Irvine, California) was used to prepare total genomic DNA of pseudoflower isolates NRRL 62710, 62721, and 66890 (TABLE 2) for whole-genome sequencing on a MiSeq system (Illumina, San Diego, California). DNA libraries with an average insert size of

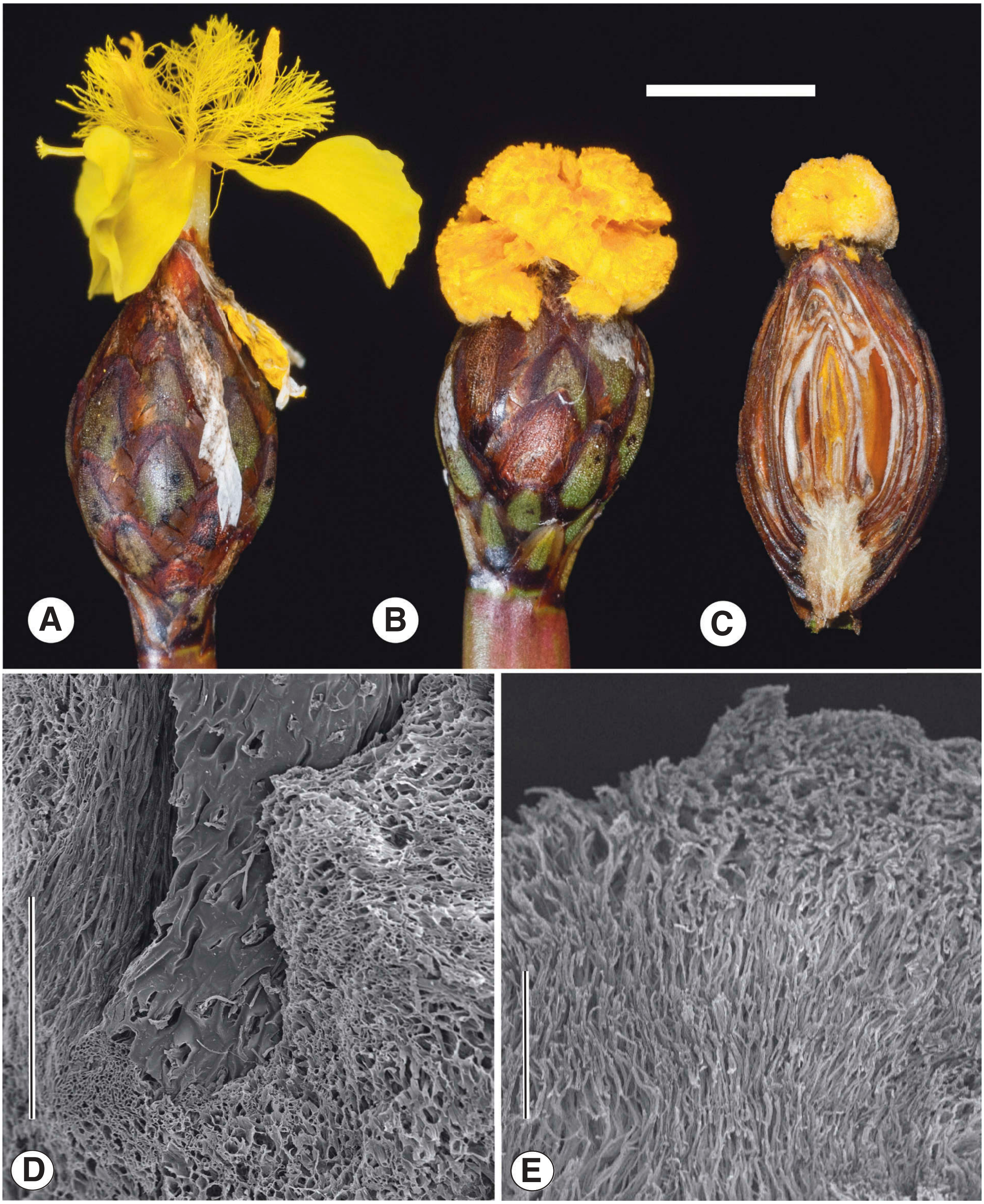

Figure 1. A. Healthy *Xyris surinamensis* flower on brown cone-like spike (inflorescence). B. Pseudoflower produced by *Fusarium xyrophilum* on *X. surinamensis* spike. C. Longitudinal section of *X. surinamensis* spike and pseudoflower of *F. xyrophilum*. D. SEM of cyrofractured pseudoflower surrounding *X. surinamensis* inflorescence. E. SEM of cyrofractured pseudoflower on *X. surinamensis* composed of textura prismatica tissue. All from KJW 5226 collected in Guyana 2010. Bars: A–C = 5 mm; D–E = 200 µm.

300 bp were prepared using a Nextera XT kit (Illumina). MiSeq sequence reads (average length 194 bases) were processed and assembled using CLC Genomics Workbench 12 (CLC bio; Qiagen, Aarhus, Denmark) using default settings except that reads were screened for contamination against Nextera adapter and 84 bacterial

Table 1. *Xyris* specimens bearing pseudoflowers collected in Guyana.

KJW no.[a]	Host	Geographic origin	Date collected	*F. xyrophilum* cultured[b]
5502	*Xyris surinamensis*	Cuyuni-Mazaruni, Guyana	July 2010	No
5508	*Xyris setigera*	Cuyuni-Mazaruni, Guyana	July 2010	No
5226	*Xyris surinamensis*	Cuyuni-Mazaruni, Guyana	July 2010	No
5664	*Xyris setigera*	Cuyuni-Mazaruni, Guyana	May 2012	Yes
5665	*Xyris surinamensis*	Cuyuni-Mazaruni, Guyana	May 2012	Yes

[a]KJW, Kenneth J. Wurdack specimen numbers.
[b]See TABLE 2.

Table 2. *Fusarium* strains included in study.

NRRL no.[a]	KOD no.[b]	KJW no.[c]	Host	Date collected	Mating type[d]
62710	116	5664	*Xyris setigera*	May 2012	*MAT1-2*
62711	117	5664	*X. setigera*	May 2012	*MAT1-2*
62712	118	5664	*X. setigera*	May 2012	*MAT1-2*
62713	119	5664	*X. setigera*	May 2012	*MAT1-2*
66890	583	5664	*X. setigera*	May 2012	*MAT1-2*
66891	584	5664	*X. setigera*	May 2012	*MAT1-2*
	585	5664	*X. setigera*	May 2012	*MAT1-2*
	586	5664	*X. setigera*	May 2012	*MAT1-2*
	587	5664	*X. setigera*	May 2012	*MAT1-2*
	588	5664	*X. setigera*	May 2012	*MAT1-2*
	589	5664	*X. setigera*	May 2012	*MAT1-2*
	591	5664	*X. setigera*	May 2012	*MAT1-2*
	592	5664	*X. setigera*	May 2012	*MAT1-2*
	593	5664	*X. setigera*	May 2012	*MAT1-2*
	594	5665	*X. surinamensis*	May 2012	*MAT1-1*
	595	5665	*X. surinamensis*	May 2012	*MAT1-1*
62721	596	5665	*X. surinamensis*	May 2012	*MAT1-1*
62722	597	5665	*X. surinamensis*	May 2012	*MAT1-1*
	598	5665	*X. surinamensis*	May 2012	*MAT1-1*
	599	5665	*X. surinamensis*	May 2012	*MAT1-1*

[a]NRRL, Agricultural Research Service Culture Collection, National Center for Agricultural Utilization Research, Peoria, Illinois.
[b]KOD, strains available from Kerry O'Donnell.
[c]KJW, Kenneth J. Wurdack specimen numbers.
[d]Determined using published PCR assay for *MAT* idiomorph (Kerényi et al. 2004).

genome sequences prior to de novo assembly. The whole-genome sequences of *F. xyrophilum* were deposited in GenBank as VYXA00000000, VYWZ00000000, and VYWY00000000.

The BLASTn application in CLC bio was used to mine full-length *RPB1, RPB2*, and *TEF1* sequences from the *F. xyrophilum* genomes and from the genomes of 21 closely related species within the *F. fujikuroi* species complex (FFSC; O'Donnell et al. 1998). Sequences of *F. gaditjirrii* NRRL 45417, *F. lyarnte* NRRL 54252, *F. nisikadoi* NRRL 25179, and *F. miscanthi* NRRL 26231 within the *F. nisikadoi* species complex (FNSC) were selected as the outgroup based on more inclusive analyses (O'Donnell et al. 2013). ModelFinder (Kalyaanamoorthy et al. 2017) identified TNe+I+G4, TIM2e+I+G4, and TIM3+F+I +G4 as the best-fit models of molecular evolution for *RPB1, RPB2*, and *TEF1*, respectively, using the Bayesian information criterion scores (Chernomor et al. 2016). Based on 5000 maximum likelihood (ML) bootstrap (BS) pseudoreplicates of the individual partitions, which did not reveal any conflict between strongly supported nodes, the *RPB1, RPB2*, and *TEF1* sequences were analyzed as a combined data set with IQ-TREE 1.6.10 (Nguyen et al. 2015; http://www.iqtree.org/). The new full-length *RPB1, RPB2*, and *TEF1* sequences analyzed in the present study were deposited in GenBank (accession nos. MN193854–MN193937), and the three-locus aligned data set and ML tree inferred with IQ-TREE were deposited in TreeBASE (accession nos. S24820, Tr119052).

Morphological characterization.—*Fusarium xyrophilum* isolates NRRL 62710, 62721, and 66891 (TABLE 2) were grown under an alternating 12 h dark/12 h near-ultraviolet (UV) black-and-white fluorescent light cycle (IntellusUltra C8; Percival Scientific, Perry, Iowa) and in the dark at 25 C on potato dextrose agar (PDA; Difco, Detroit, Michigan) to characterize colony morphology, odor, and color using Kornerup and Wanscher (1978) as the color guide. Strains were grown in the dark on PDA in triplicate at six different temperatures (10, 15, 20, 25, 30, and 35 C) to determine the optimal temperature for mycelial growth. By measuring 16 radii around the colony margin, radial growth in mm/d was determined 1, 5, and 17 d post inoculation using ImageJ 1.51 software (https://imagej.nih.gov/ij/) as reported previously (Aoki et al. 2015). Strains were grown on synthetic low-nutrient agar (SNA; Nirenberg 1976) overlaid with pieces of sterile filter paper, carnation leaf agar (CLA; Fisher et al. 1982), and mung bean agar (MBA; Dill-Macky 2003) under an alternating 12 h dark/12 h near-UV black-and-white fluorescent light cycle at 25 C to obtain detailed morphological data. Strains were also grown on soil extract agar (SEA; Klotz et al. 1988) to determine whether they could produce chlamydospores. Light microscopy was conducted using a Zeiss Axioplan microscope (Jena, Germany) and imaged with a Jenoptik ProgRes CCD (charged-couple device) camera using CapturePro 2.8.8 software. Differential interference contrast (DIC) light micrographs were obtained from water mounts using a Plan-Neofluar 40×/0.75 objective, and a dark-field image of synnemata was acquired using a Planapo 10×/0.32 objective. Samples for SEM of strains cultured on SNA and CLA were fixed with 2% aqueous OsO_4 vapors overnight in the dark, and then they were dehydrated in a graded ethanol series following a published protocol (Laraba et al. 2018). The samples were then dried in a Samdri-PVT-3D critical point dryer, coated with gold in a SPI sputter coater, and then imaged using a JEOL JSM-6010A scanning electron microscope.

Mating type idiomorph and sexual crosses.—Fourteen single-conidial isolates recovered from pseudoflowers on *X. setigera* and six isolates from *X. surinamensis* were screened for *MAT* idiomorph using a published uniplex PCR assay (Kerényi et al. 2004). In addition, the BLASTn application in CLC Genomics Workbench was used to search the NRRL 62710, 62721, and 66890 genomes for the mating type locus (*MAT*). Once *MAT* idiomorph was determined, the *MAT1-1* and *MAT1-2* isolates were tested for female fertility by individually crossing them with two isolates of the opposite mating type, which were used as males as previously described (Zhou et al. 2018). Briefly, isolates were grown on half-strength carrot agar under an alternating 12 h dark/12 h near-UV black-and-white fluorescent light cycle (IntellusUltra C8; Percival Scientific) at 25 C. After incubation for 3 wk, conidia of each *MAT1-1* and *MAT1-2* male parent were harvested in 0.2% Tween 20, and then 1 mL of each conidial suspension was spread over a 1-wk-old strain of the opposite mating type that was used as the female parent. Once the crosses were set, they were incubated at 18, 22, and 25 C under an alternating 12 h dark/12 h near-UV black-and-white fluorescent light cycle for 10 wk.

Secondary metabolite biosynthetic potential.—The BLASTn application in CLC Genomics Workbench was used to examine the occurrence of genes required for biosynthesis of mycotoxins, plant hormones, pigments, and other secondary metabolites in the genome sequences of *F. xyrophilum* strains NRRL 62710, 62721, and 66890. The queries used in the analysis were previously described sequences of secondary metabolite biosynthetic genes from other *Fusarium* species (Niehaus et al. 2016; Laraba et al. 2018).

Secondary metabolite production in culture.—Strains of *F. xyrophilum* were grown on a solid cracked maize kernel medium for 28 d in the dark at 25 C to assess their ability to produce mycotoxins and other biologically active metabolites (Aoki et al. 2015; Laraba et al. 2018). After the 28-d incubation period, 10 g of each culture was extracted with 50 mL acetonitrile-water (86:14 vol/vol), the extracts were passed through Whatman 2CV filters (GE Healthcare UK, Amersham, Buckinghamshire, UK), and then they were analyzed by liquid chromatography–mass spectrometry (LC-MS) using a Dionex model U3000 high-performance liquid chromatography instrument connected to a QTRAP 3200 tandem mass spectrometer (AB SCIEX, Thornhill, Ontario, Canada). The extracts were also separated on a C18 column (Kinetex XB-C18 50 × 2.1 mm; Phenomenex, Torrance, California) by eluting them with a methanol/water gradient (0.6 mL/min, 20–95% methanol over 5 min), followed by MS detection with electrospray ionization in positive and negative ionization modes. Compounds were identified by comparing ion mass, elution time, and ion fragmentation with purified standards and a MS reference library (Busman et al. 2012; Busman 2017).

RESULTS

Host collections and fungal isolates.—During botanical field work conducted in 2010 and 2012 on the upland savannas in the Pakaraima Mountains of Guyana, yellow-orange pseudoflowers were observed repeatedly on the inflorescences of two *Xyris* species, *X. setigera* and *X. surinamensis*, and once on *X. bicephala*. The visual similarity between the host flowers and pseudoflowers was striking (FIG. 1A–C). Scanning electron microscope images, however, indicated that the pseudoflowers were entirely fungal and composed of textura prismatica tissue (FIG. 1D–E). Efforts to isolate pure cultures from pseudoflowers collected in 2012 resulted in 14 single-conidial isolates from *X. setigera* and 6 from *X. surinamensis* (TABLE 2). These isolates appeared to be conspecific based on identical *TEF1* sequences from the 5′ end of this gene.

Molecular phylogenetics and whole-genome sequencing.—BLASTn searches of GenBank, using the ITS rDNA and partial sequence from the 3′ end of the *TEF1* gene as the queries, indicated that the petaloid structures contained *Fusarium*; however, a species-level identification was not possible with these conserved sequences. Therefore, BLASTn searches of National Center for Biotechnology Information (NCBI) GenBank were conducted, using the partial sequence from the intron-rich 5′ end of *TEF1* of NRRL 62710, 62721, and 66890 as the queries. These searches indicated that the highest levels of nucleotide sequence identity (92–93%) were to *Fusarium nygamai* and *F. pseudocircinatum*, which are members of the African clade of the FFSC. However, the relatively low levels of sequence identity, and reciprocal monophyly with *F. pseudocircinatum* in the individual partitions (SUPPLEMENTARY FIG. 1) and combined data set, suggested that the pseudoflower isolates represented a novel species of *Fusarium*, hereafter referred to as *F. xyrophilum*. In order to accurately infer its evolutionary relationships within the FFSC, full-length sequences of *RPB1* (5365 bp alignment, 596 parsimony-informative characters [PICs]), *RPB2* (3914 bp alignment, 453 PICs), and *TEF1* (1790 bp alignment, 177 PICs) totaling 11 069 bp (1226 PICs) were mined from whole-genome sequences of *F. xyrophilum* NRRL 62710, 62721, and 66890, 21 other species within the FFSC, and 4 representative species of the FNSC. Partitioned ML analyses of the combined three-locus data set strongly supported the genealogical exclusivity of *F. xyrophilum* (ML-BS = 100%; FIG. 2) within the African clade of the FFSC. The ML analysis also resolved a sister-group relationship of *F. xyrophilum* and *F. pseudocircinatum* NRRL 36939 (ML-BS = 100%; FIG. 2). These two species were in turn resolved as sisters to *F. lactis* NRRL 25200 (ML-BS = 99%; FIG. 2). In addition, the African, Asian, and American clades of the FFSC were strongly supported as monophyletic (ML-BS = 100%; FIG. 2).

Mating type idiomorph and sexual crosses.—Results of the PCR assay for determining *MAT* idiomorph revealed that the 20 single-conidial isolates of *F. xyrophilum* recovered from pseudoflowers possessed either a *MAT1-1* or *MAT1-2* idiomorph. The 6 isolates recovered from *X. surinamensis* and 14 from *X. setigera* were *MAT1-1* and *MAT1-2*, respectively (TABLE 2). Analysis of genome sequences revealed that *F. xyrophilum* NRRL 62710 and 66890 had the *MAT1-2* idiomorph, whereas *F. xyrophilum* NRRL 62721 had the *MAT1-1* idiomorph. To determine whether *F. xyrophilum* could reproduce sexually, we subjected *MAT1-1* and *MAT1-2* strains to a standard

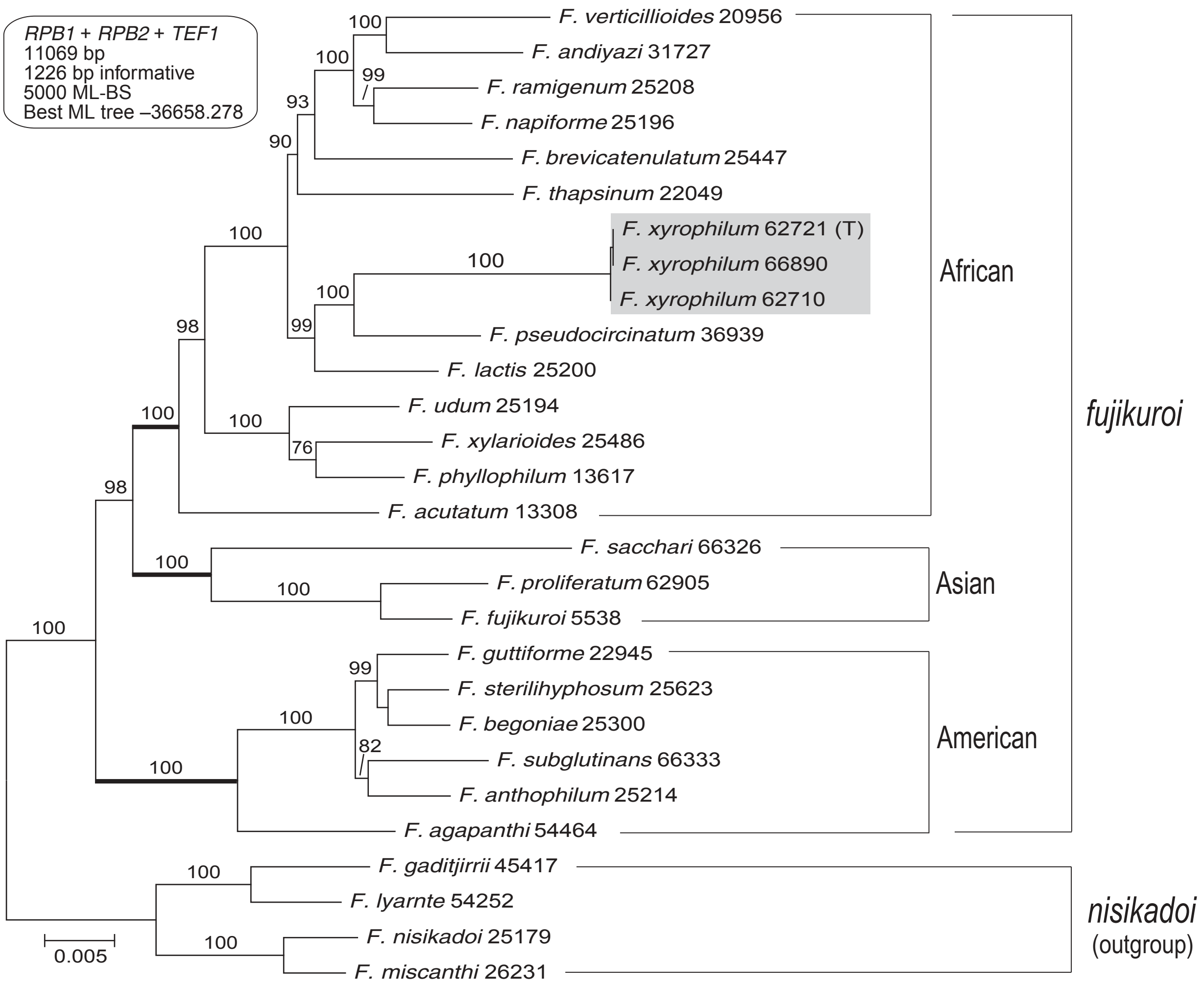

Figure 2. Partitioned maximum likelihood bootstrap (ML-BS) analysis of three-locus data set of the *Fusarium fujikuroi* species complex (FFSC) conducted using IQ-TREE 1.6.5. The FFSC was rooted on sequences of its sister group, the *F. nisikadoi* species complex. Numbers above nodes represent ML-BS support based on 5000 pseudoreplicates. *Fusarium xyrophilum* (gray highlight) was resolved as sister to *F. pseudocircinatum* within the African clade of the FFSC. The African, Asian, and American clades of the FFSC (identified by thickened internodes) were strongly supported as monophyletic (ML-BS = 100%). Each strain is identified by an ARS Culture Collection (NRRL) number. The log-likelihood of the best tree was −36658.278. T = type strain.

Fusarium mating assay using half-strength carrot agar and three incubation temperatures (18, 22, and 25 C). None of the attempted matings resulted in the formation of perithecia after 10 wk of incubation.

Secondary metabolite biosynthetic potential.— Analyses of genome sequences indicated that *F. xyrophilum* has the genetic potential to produce multiple secondary metabolites, including mycotoxins, pigments, and phytohormones. The genomes included intact gene clusters required for biosynthesis of the mycotoxin beauvericin, the siderophore ferricrocin, as well as fusarubin and carotenoid pigments. The genomes also possessed homologs of the two-gene loci required for production of auxins and cytokinins and contained six of the seven gibberellin cluster genes, one of which was pseudogenized. However, the cluster still had potential to confer production of multiple gibberellin analogs (TABLE 3). By contrast, the *F. xyrophilum* genomes lacked homologs of gene clusters responsible for production of several mycotoxins (e.g., fumonisins, zearalenone, and trichothecenes). The genomes also included partial and presumably nonfunctional gene clusters responsible for production of other secondary metabolites (e.g., bikaverin, equisetin, and fusaric acid) (TABLE 3).

Table 3. Secondary metabolite biosynthetic gene clusters in *F. xyrophilum* genomes.

Metabolite	NRRL 62710	NRRL 62721	NRRL 66890
Alpha-acorenol	$+^{*}$	$+^{*}$	$+^{*}$
Apicidin	–	–	–
Aurofusarin	$+^{*}$	$+^{*}$	$+^{*}$
Auxin	+	+	+
Beauvericin	+	+	+
Bikaverin	$+^{*}$	$+^{*}$	$+^{*}$
Carotenoid	+	+	+
Culmorin	–	–	–
Cytokinins	+	+	+
Depudecin	$+^{*}$	$+^{*}$	$+^{*}$
Equisetin	$+^{*}$	$+^{*}$	$+^{*}$
Ferricrocin	+	+	+
Fujikurin	–	–	–
Fumonisin	–	–	–
Fumosorinone	–	–	–
Fusaric acid	$+^{*}$	$+^{*}$	$+^{*}$
Fusaridione	–	–	–
Fusarielin	$+^{*}$	$+^{*}$	$+^{*}$
Fusarin C	$+^{P}$	$+^{P}$	$+^{P}$
Fusarinine	$+^{*}$	$+^{*}$	$+^{*}$
Fusaristatin	$+^{*}$	$+^{*}$	$+^{*}$
Fusarubin	+	+	+
Geranylgeranyl diphosphate synthases	+	+	+
Gibberellin	$+^{P}$	$+^{P}$	$+^{P}$
Gibepyron	$+^{P}$	$+^{P}$	$+^{P}$
Malonichrome	$+^{*}$	$+^{*}$	$+^{*}$
Orcinol	$+^{*}$	$+^{*}$	$+^{*}$
Pyripyropene	$+^{*}$	$+^{*}$	$+^{*}$
Eremophilene	$+^{*}$	$+^{*}$	$+^{*}$
Guaia-6,10(14)-diene	$+^{*}$	$+^{*}$	$+^{*}$
Trichothecene	–	–	–
W493	$+^{*}$	$+^{*}$	$+^{*}$
Zearalenone	–	–	–

+ = Gene cluster complete.
– = Gene cluster absent.
$+^{*}$ = Only some cluster genes are present. However, based on functional analyses in other *Fusarium* species, the genes that are present are not sufficient for production of the corresponding metabolite.
$+^{P}$ = Some fusarin, gibberellin, and gibepyron cluster genes are present. Although these genes are not sufficient for production of these metabolites, they should be sufficient for production of some of biosynthetic intermediates, based on functional analyses of the genes in *F. fujikuroi*.

Secondary metabolite production in culture.— *Fusarium xyrophilum* strains were tested for their ability to produce multiple secondary metabolites in a solid cracked maize kernel medium using a LC-MS system. Result of the analysis indicated that none of the strains produced detectable levels of moniliformin, fusaric acid, fumonisins (FB1, FB2, FB3), and the pigment bikaverin. The genome analysis indicated that *F. xyrophilum* has an intact fusarubin biosynthetic gene cluster. Consistent with this finding, the LC-MS analysis detected the pigment 8-*O*-methylbostrycoidin, which is a product of the fusarubin biosynthetic pathway. The beauvericin/enniatin biosynthetic gene cluster was also present in the three *F. xyrophilum* genome sequences, but none of the strains analyzed produced detectable levels of these metabolites (SUPPLEMENTARY TABLE 1).

TAXONOMY

Fusarium xyrophilum I. Laraba, K.J. Wurdack, Aime & O'Donnell, sp. nov. FIGS. 3–4
MycoBank MB830986

Typification: GUYANA. CUYUNI-MAZARUNI: Below 1st escarpment (of four) of Kamakusa Mountain, Partang Airstrip (presently nonoperational) and vicinity, white sand savanna mixed with flat sandstone rock outcrops and scrub, 5°48′55″N, 60°13′32″W, 734 m, from *Xyris surinamensis* vouchered as KJW 5665, 19 May 2012, *K.J. Wurdack* (**holotype** BPI 910919, dried culture of NRRL 62721). Ex-type culture NRRL 62721 = FRC M-8921.

Etymology: Xyro- (Greek), razor, referring to *Xyris* and its two-edged leaf form and -philum (Greek), loving, referring to the host association.

Observations on PDA: Colony surface in the dark initially white (1A1) becoming dark purple (14F4) with age, colony reverse purplish gray (14F2); abundant white (1A1) aerial mycelium produced at colony margin. Under an alternating 12 h dark/12 h near-UV black-and-white fluorescent light cycle, colony surface with concentric yellow (3A6) to brownish orange (6C8) rings, colony reverse purplish gray (14F2); aerial mycelium sparse throughout colony. Brownish orange (8C3) pigment diffused in agar when incubated in dark and under an alternating 12 h dark/12 h near-UV black-and-white fluorescent light

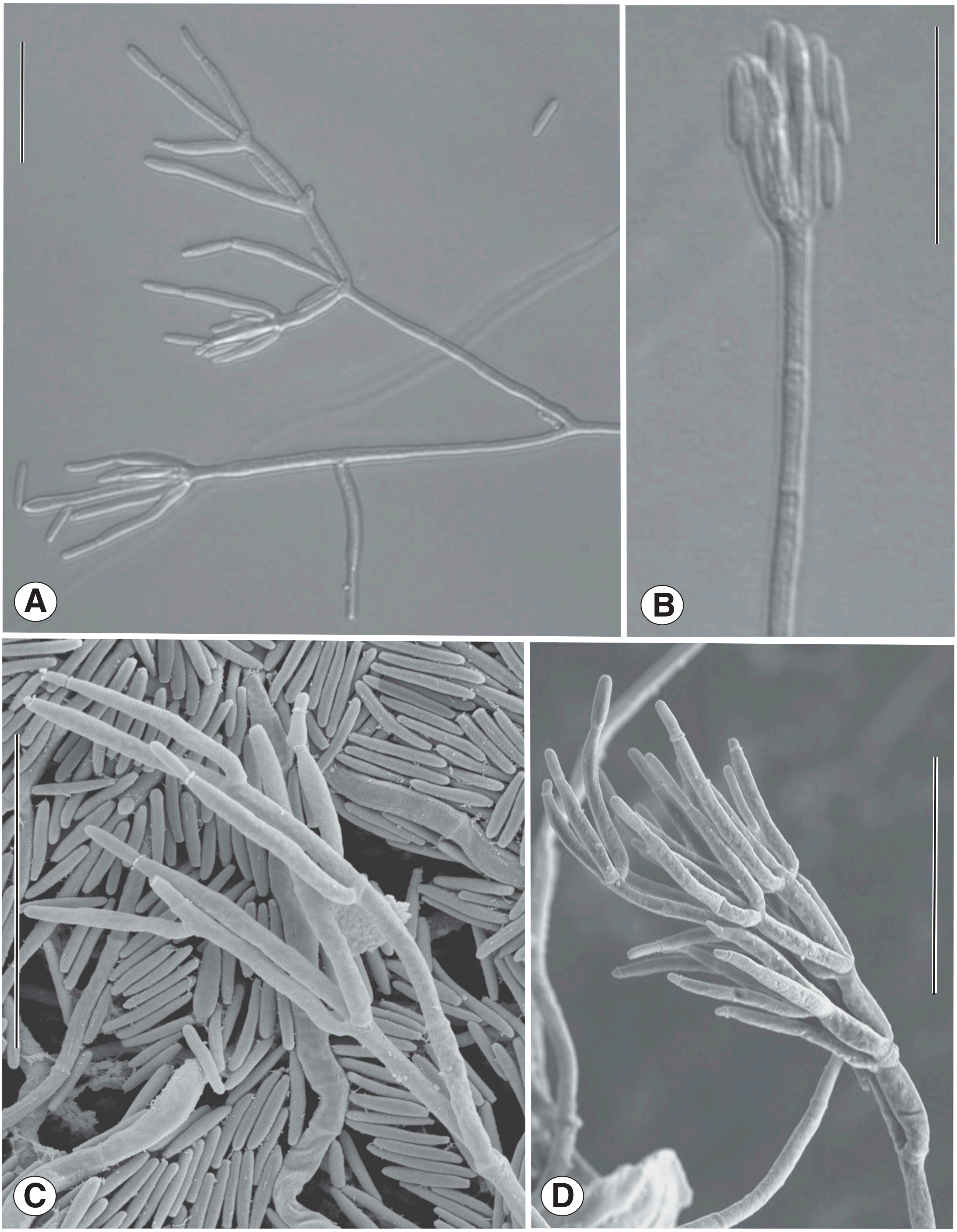

Figure 3. *Fusarium xyrophilum* NRRL 62721 cultured on CLA at 25 C under a 12 h dark/12 h near-UV black-and-white fluorescent light cycle. A. DIC light micrograph of mostly verticillately branched aerial conidiophore producing oblong to cylindrical, 0-septate conidia on monophialides. B. Conidiophore bearing oblong to clavate, 0-septate conidia in a false head. C. SEM of sympodially and verticillately branching aerial conidiophore producing 0-septate conidia from monophialides that possess a distinct collarette. D. SEM of verticillately branched aerial conidiophore producing oblong conidia from monophialides. Bars: A–D = 25 μm.

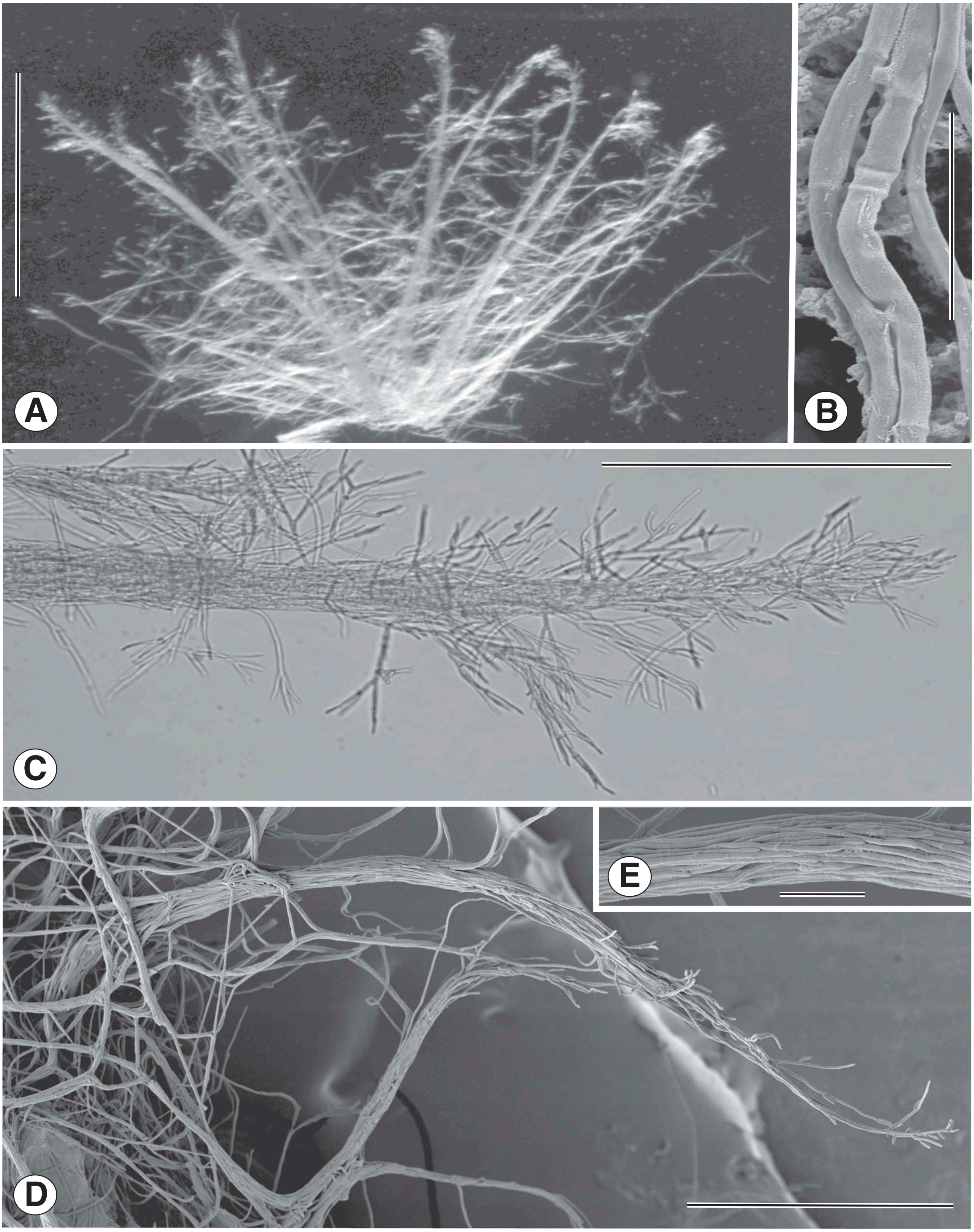

Figure 4. *Fusarium xyrophilum* NRRL 62721 cultured under a 12 h dark/12 h near-UV black-and-white fluorescent light cycle at 25 C on CLA. A. Dark-field light micrograph of synnemata excised from a carnation leaf on CLA. B. SEM showing hyphal fusions between parallel vegetative hyphae. C. Phase-contrast light micrograph of apical portion of synnema shown just to right of scale bar in A. D. SEM of synnemata produced on CLA. E. Enlarged central portion of synnema in D showing compact bundle of parallel conidiophores. Bars: A = 1 mm; B, E = 25 μm; C–D = 0.25 mm.

cycle. Colony odor moldy. Sporodochia, sclerotia, and multiseptate conidia not observed. Colony margin entire with optimal average radial growth rate 4.7–5.3 mm/d at 25 C. No colony growth at 5, 10, and 35 C. On CLA and SNA with filter paper: Sporulation under alternating 12 h dark/12 h near-UV black-and-white fluorescent light observed after 3 wk. Aerial conidiophores originating from agar unbranched or branched irregularly, dichotomously, verticillately or sympodially. Phialides of aerial conidiophores monophialidic, hyaline, ampulliform to subcylindrical, (8–)13–23(–23.5) × (1.5–)2–3(–3.5) µm, average ± SD 16 ± 1 × 2 ± 0.1 µm (n = 40), producing hyaline, oblong to cylindrical, 0-septate conidia, (5.5–)7–9(–14.5) × (1.5–)1.5–2(–2.5) µm, average ± SD 8.5 ± 0.27 × 2 ± 0.04 µm (n = 50), accumulated in false heads mostly produced within mung bean agar. Indeterminate synnemata up to 2 mm tall produced abundantly on carnation leaves; synnema composed of parallel bundles of densely packed conidiophores, branched dichotomously or verticillately, terminating in hyaline, subcylindrical to navicular monophialides, (10–)-14–21.5(–23.5) × (1.5–)1.5–2.5(–3) µm, average ± SD 15.5 ± 0.51 × 2 ± 0.06 µm (n = 40), bearing hyaline, oblong to cylindrical, 0-septate conidia, (5–)7.5–10(–13) × (1–)1.5–2 (–2.5) µm, average ± SD 9 ± 0.20 × 2 ± 0.03 µm (n = 50). Anastomoses between substrate mycelium common on SNA and CLA. Chlamydospores not observed.

Distribution: Guyana.

Notes: Fusarium xyrophilum can be distinguished from all other described fusaria by a unique combination of characters, including production of pseudoflowers on at least three perennial species of *Xyris* in northern South America, production of oblong to cylindrical, 0-septate microconidia from monophialides on erect indeterminate synnemata produced on carnation leaves and in false heads mostly embedded in mung bean agar, yellow to brownish orange colonies on PDA under an alternating 12 h dark/12 h near-UV black-and-white fluorescent light cycle, and as sister to *F. pseudocircinatum* in the three-locus molecular phylogeny (FIG. 2).

Additional strains examined: See TABLE 2.

DISCUSSION

This study reports on the discovery and characterization of a unique floral mimicry system caused by a novel *Fusarium* species that produces pseudoflowers on the sterilized inflorescences of *X. setigera* and *X. surinamensis* in Guyana. The yellow-orange flower-like structures were also observed on the inflorescences of *X. bicephala*. These hosts have broader distributions across northern South America, and *F. xyrophilum* is expected to follow these ranges, which has been partly confirmed with herbarium surveys documenting limited additional pseudoflower records (Laraba et al., unpublished data). This fungus appears to inhibit the development of normal flowers and produces unique pseudoflowers made up of fungal tissues that mimic *Xyris* flowers in color, shape, and size. DNA sequence–based phylogenetic analyses indicated that the pseudoflower-inducing fungus was a novel *Fusarium* species within the African clade of the FFSC that we formally described here as *F. xyrophilum*. Our results also provide strong support for a sister-group relationship of *F. xyrophilum* and *F. pseudocircinatum. Fusarium xyrophilum* can be diagnosed by a unique combination of characters: it is the only *Fusarium* species known to produce synnemata, it apparently lacks the ability to produce iconic multiseptate fusiform macroconidia, and it only produces 0-septate microconidia from monophialides on indeterminate synnemata or in false heads. To our knowledge, the present study represents the first report of *Fusarium* on *Xyris*. Because *F. xyrophilum* apparently does not produce macroconidia, it might have been described previously as a species of *Tilachlidium* (Seifert et al. 2011). However, we were unable to find any reports of *Tilachlidium* on *Xyris*.

Results of the *MAT* PCR assay revealed that single-conidial strains of *F. xyrophilum* contain a *MAT1-1* or *MAT1-2* idiomorph, which suggests that this fungus has the genetic potential for a heterothallic sexual reproductive mode. Therefore, the failure of *F. xyrophilum* strains to cross on carrot agar might be because the experimental conditions employed were suboptimal or the strains are not female-fertile. Low percentages of female-fertile isolates have been reported in several species within the FFSC (Covert et al. 1999; Steenkamp et al. 2000; Zeller et al. 2003).

Species within the FFSC differ considerably in the presence of secondary metabolite biosynthetic gene clusters and in their ability to produce secondary metabolites (Niehaus et al. 2016). As noted for some other members of the FFSC (Kim et al. 2017), complete gene clusters required for synthesis of beauvericin/enniatins, ferricrocin, fusarubin, and carotenoids were present in the genome of *F. xyrophilum*. However, 8-*O*-methylbostrycoidin, a product of the fusarubin biosynthetic pathway, was the only secondary metabolite detected in cracked maize kernel culture extracts of *F. xyrophilum*. Although some of the genes required for the biosynthesis of bikaverin, equisetin, fusaric acid, among others (TABLE 3), were present in the *F. xyrophilum* genomes, the absence of other genes essential for production of these metabolites should preclude production (Brown et al. 2012, 2015). As is the case for some other members of the FFSC, *F. xyrophilum* genomes analyzed in this study contained gene clusters required for synthesis of three classes of plant hormones: auxins, cytokinins, and gibberellins. Several FFSC species (*F. fujikuroi, F. proliferatum, F. verticllioides, F. mangiferae*, and

F. oxysporum) possess a two-gene cluster consisting of bacterium-like homologs of the genes *IAAM* and *IAAH*, which confer the ability to convert tryptophan to the auxin IAA via an indole-3-acetamide (IAM) intermediate (Tsavkelova et al. 2012; Niehaus et al. 2016; Kim et al. 2017). All three *F. xyrophilum* genomes examined had one homolog of the indole-3-acetic acid (IAA) biosynthetic gene cluster. Recent comparative genomic analyses provided evidence that another two-gene cluster, consisting of the *IPTLOG1* and *P450-1* genes, confers the ability to produce cytokinins in multiple members of the FFSC (Niehaus et al. 2016; Kim et al. 2017; Vrabka et al. 2019). Most of these fungi have two paralogs of this latter cluster. However, the *F. xyrophilum* strains examined here only had one homolog of the cytokinin cluster. The gibberellin cluster in the *F. xyrophilum* genomes was incomplete because the desaturase gene, *DES*, was absent and the 13-hydroxylase gene, *P450-3*, was pseudogenized. The absence of functional versions of *DES* and *P450-3* should preclude production of the gibberellin analogs GA_1, GA_3, and GA_7 based on functional analyses in *F. fujikuroi*. However, *DES* and *P450-3* are not required for production of the gibberellin analogs GA_4, GA_9, GA_{12}, and GA_{14} (Bömke and Tudzynski 2009).

Fusarium xyrophilum can be diagnosed phenotypically; however, because it doesn't produce iconic fusiform macroconidia and only produces 0-septate microconidia on synnemata and/or in false heads, molecular systematic data were essential for accurate placement in *Fusarium* and the FFSC. Fortunately, two online databases dedicated to the identification of unknown fusaria, FUSARIUM-ID (http://isolate.fusariumdb.org/blast.php; Geiser et al. 2004) and *Fusarium MLST* (http://www.westerdijkinstitute.nl/fusarium/), are populated with portions of *TEF1*, *RPB1*, and *RPB2*, which are phylogenetically informative at or near the species level (O'Donnell et al. 2015).

In summary, we discovered and formally described a novel *Fusarium* species that produces pseudoflowers on several perennial *Xyris* species in northern South America. In contrast to the floral mimicry systems described for *Monilinia* (Batra and Batra 1985; McArt et al. 2016), *Puccinia* (Roy 1993), and *Uromyces* (Pfunder and Roy 2000), where the flower-like structures are modified leaves, those on *Xyris* are composed exclusively of *Fusarium*. Results of the present study lay the taxonomic framework and provide a starting point for investigating the evolutionary ecology and molecular biology of a spectacular floral mimicry system.

ACKNOWLEDGMENTS

The authors thank Gail Doehring, Amy McGovern, Nathane Orwig, and Deborah S. Shane for skilled technical assistance. The authors also thank Mark Strong (SI) for the *Xyris* identifications. The authors are also indebted to the reviewers and associate editor for numerous suggestions for improving this submission.

FUNDING

The US Department of Agriculture Agricultural Research Service (USDA-ARS) National Program for Food Safety and National Science Foundation (NSF; DEB-1655980) provided funding for this study. This research was supported in part by an appointment to the ARS Research Participation Program administered by the Oak Ridge Institute for Science and Education (ORISE) through an interagency agreement between the US Department of Energy (DOE) and the US Department of Agriculture (USDA). ORISE is managed by ORAU under DOE contract number DE-SC0014664. All opinions expressed in this paper are the authors' and do not necessarily reflect the policies and views of USDA, DOE, or ORAU/ORISE. Field work by Kenneth J. Wurdack was supported by the National Geographic Society/Waitt Grants Program (Karen Redden, Principal Investigator) and the Biological Diversity of the Guiana Shield Program, Smithsonian Institution.

DISCLAIMER

ORCID

Mark Busman http://orcid.org/0000-0001-9750-064X
Kerry O'Donnell http://orcid.org/0000-0001-6507-691X
Frederick C. Felker http://orcid.org/0000-0002-5311-7697
Rachel A. Koch http://orcid.org/0000-0001-7240-1303

LITERATURE CITED

Aoki T, Vaughan MM, McCormick SP, Busman M, Ward TJ, Kelly A, O'Donnell, K, Johnston PR, Geiser DM. 2015. *Fusarium dactylidis* sp. nov., a novel nivalenol toxin-producing species sister to *F. pseudograminearum* isolated from orchard grass (*Dactylis glomerata*) in Oregon and New Zealand. Mycologia 107:409–418.

Batra LR, Batra SWT. 1985. Floral mimicry induced by mummy-berry fungus exploits host's pollinators as vectors. Science 228:1011–1013.

Bömke C, Tudzynski B. 2009. Diversity, regulation, and evolution of the gibberellin biosynthetic pathway in fungi compared to plants and bacteria. Phytochemistry 70:1876–1893.

Brown DW, Butchko RA, Busman M, Proctor RH. 2012. Identification of gene clusters associated with fusaric acid, fusarin, and perithecial pigment production in *Fusarium verticillioides*. Fungal Genetics and Biology 49:521–532.

Brown DW, Lee SH, Kim LH, Ryu JG, Lee S, Seo Y, Kim YH, Busman M, Yun SH, Proctor RH, Lee T. 2015. Identification of a 12-gene fusaric acid biosynthetic gene cluster in *Fusarium* species through comparative and functional genomics. Molecular Plant-Microbe Interactions 28:319–332.

Busman M. 2017. Utilization of high performance liquid chromatography coupled to tandem mass spectrometry for characterization of 8-*O*-methylbostrycoidin production by species of the fungus *Fusarium*. Journal of Fungi 3:43.

Busman M, Butchko RA, Proctor RH. 2012. LC-MS/MS method for the determination of the fungal pigment bikaverin in maize kernels as an indicator of ear rot. Food Additives & Contaminants: Part A 29:1736–1742.

Chase MW, Hills HH. 1991. Silica gel: an ideal material for field preservation of leaf samples for DNA studies. Taxon 40:215–220.

Chernomor O, von Haeseler A, Minh BQ. 2016. Terrace aware data structure for phylogenomic inference from supermatrices. Systematic Biology 65:997–1008.

Covert SF, Briley A, Wallace MM, McKinney VT. 1999. Partial *MAT-2* gene structure and the influence of temperature on mating success in *Gibberella circinata*. Fungal Genetics and Biology 28:43–54.

Dill-Macky R. 2003. Inoculation methods and evaluation of Fusarium head blight resistance in wheat. In: Leonard KJ, Bushnell WR, eds. Fusarium head blight in wheat and barley. St. Paul, Minnesota: The American Phytopathological Society Press. p. 184–210.

Edgar RC. 2004. MUSCLE: multiple sequence alignment with high accuracy and high throughput. Nucleic Acids Research 32:1792–1797.

Fisher NL, Burgess LW, Toussoun TA, Nelson PE. 1982. Carnation leaves as a substrate and for preserving cultures of *Fusarium* species. Phytopathology 72:151–153.

Gardes M, Bruns TD. 1993. ITS primers with enhanced specificity for basidiomycetes—application to the identification of mycorrhizae and rusts. Molecular Ecology 2:113–118.

Geiser DM, del Mar Jiménez-Gasco, Kang S, Makalowska I, Veeraraghavan N, Ward TJ, Zhang N, Kuldau GA, O'Donnell K. 2004. FUSARIUM-ID v. 1.0: a DNA sequence database for identifying *Fusarium*. European Journal of Plant Pathology 110:473–479.

Gouy M, Guindon S, Gascuel O. 2009. SeaView version 4: a multiplatform graphical user interface for sequence alignment and phylogenetic tree building. Molecular Biology and Evolution 27:221–224.

Gronquist M, Bezzerides A, Attygalle A, Meinwald J, Eisner M, Eisner T. 2001. Attractive and defensive functions of the ultraviolet pigments of a flower (*Hypericum calycinum*). Proceedings of the National Academy of Sciences of the United States of America 98:13745–13750.

Kalyaanamoorthy S, Minh BQ, Wong TKF, von Haeseler A, Jermiin LS. 2017. ModelFinder: fast model selection for accurate phylogenetic estimates. Nature Methods 14:587–589, doi:10.1038/nmeth.4285

Kelloff CL. 2003. The use of biodiversity data in developing Kaieteur National Park, Guyana for ecotourism and conservation. Contributions to the Study of Biological Diversity 1:1–46.

Kelly AC, Clear RM, O'Donnell K, McCormick S, Turkington TK, Tekauz A, Gilbert J, Kistler HC, Busman M, Ward TJ. 2015. Diversity of fusarium head blight population and trichothecene toxin types reveals regional differences in pathogen composition and temporal dynamics. Fungal Genetics and Biology 82:22–31.

Kerényi Z, Moretti A, Waalwijk C, Oláh B, Hornok L. 2004. Mating type sequences in asexually reproducing *Fusarium* species. Applied and Environmental Microbiology 70:4419–4423.

Kim H-S, Proctor RH, Brown D. 2017. Comparative genomic analysis of secondary metabolite gene clusters in 207 isolates of *Fusarium*. In: 29th Fungal Genetics Conference; March 14–19, 2017; Pacific Grove, CA; Asilomar Conference Center. Rockville, Maryland: The Genetics Society of America. Abstract 297F, p. 170.

Klotz LV, Nelson PE, Toussoun TA. 1988. A medium for enhancement of chlamydospore formation in *Fusarium* species. Mycologia 80:108–109.

Kornerup A, Wanscher JH. 1978. Methuen handbook of color. 3rd ed. London: Methuen. 252 p.

Kral R. 1988. The genus *Xyris* (Xyridaceae) in Venezuela and contiguous northern South America. Annals of the Missouri Botanical Garden 75:522–572.

Lara C, Ornelas JF. 2003. Hummingbirds as vectors of fungal spores in *Moussonia deppeana* (Gesneriaceae): taking advantage of a mutualism? American Journal of Botany 90:262–269.

Laraba I, Keddad A, Boureghda H, Abdallah N, Vaughan MM, Proctor RH, Busman M, O'Donnell K. 2018. *Fusarium algeriense*, sp. nov., a novel toxigenic crown rot pathogen of durum wheat from Algeria is nested in the *Fusarium burgessii* species complex. Mycologia 109:935–950.

Laurence MH, Summerell BA, Burgess LW, Liew ECY. 2011. *Fusarium burgessii* sp. nov. representing a novel lineage in the genus *Fusarium*. Fungal Diversity 49:101–112.

Leslie JF, Summerell BA. 2006. The *Fusarium* laboratory manual. Ames, Iowa: Blackwell Professional Publishing. 388 p.

Marasas WFO, Ploetz RC, Wingfield MJ, Wingfield BD, Steenkamp ET. 2006. Mango malformation disease and the associated *Fusarium* species. Phytopathology 96:667–672.

McArt SH, Miles TD, Rodriguez-Saona C, Schilder A, Adler LS, Grieshop MJ. 2016. Floral scent mimicry and vector-pathogen associations in a pseudoflower-inducing plant pathogen system. PLoS ONE 11:e0165761, doi:10.1371/journal.pone.0165761

Naef A, Roy BA, Kaiser R, Honegger R. 2002. Insect-mediated reproduction of systemic infections by *Puccinia arrhenatheri* on *Berberis vulgaris*. New Phytologist 154:717–730.

Ngugi HK, Scherm H. 2006. Mimicry in plant-parasitic fungi. FEMS Microbiology Letters 257:171–176.

Nguyen L-T, Schmidt HA, von Haeseler A, Minh BQ. 2015. IQ-TREE: a fast and effective stochastic algorithm for estimating maximum likelihood phylogenies. Molecular Biology and Evolution 32:268–274, doi:10.1093/molbev/msu300

Nicholson RID, Van Staden J. 1988. Cytokinins and mango flower malformation. I. Tentative identification of the complement in healthy and malformed inflorescences. Journal of Plant Physiology 132:720–724.

Niehaus EM, Munsterkotter M, Proctor RH, Brown DW, Sharon A, Idan Y, Oren-Young L, Sieber CM, Novak O, Pencik A, Tarkowska D, Hromadova K, Freeman S, Maymon M, Elazar M, Youssef SA, El-Shabrawy EM, Shalaby ABA, Houterman P, Brock NL, Burkhardt I, Tsavkelova EA, Dickschat JS, Galuszka P, Güldener U, Tudzynski B. 2016. Comparative "omics" of the *Fusarium fujikuroi* species complex highlights differences in genetic potential and metabolite synthesis. Genome Biology and Evolution 8:3574–3599.

Nirenberg HI. 1976. Untersuchungen über die morphologische und biologische Differenzierung in der *Fusarium* Sektion Liseola. Mitteilungen aus der Biologischen Bundesanstalt für Land- und Forstwirtschaft Berlin-Dahlem 169:1–117.

O'Donnell K, Cigelnik E, Nirenberg HI. 1998. Molecular systematics and phylogeography of the *Gibberella fujikuroi* species complex. Mycologia 90:465–493.

O'Donnell K, Hooper GR. 1977. Cryofracturing as a technique for the study of fungal structures in the scanning electron microscope. Mycologia 69:309–320.

O'Donnell K, Kistler HC, Tacke BK, Casper HH. 2000. Gene genealogies reveal global phylogeographic structure and reproductive isolation among lineages of *Fusarium graminearum*, the fungus causing wheat scab. Proceedings of the National Academy of Sciences of the United States of America 97:7905–7910.

O'Donnell K, Rooney AP, Proctor RH, Brown DW, McCormick SP, Ward TJ, Frandsen RJN, Lysøe E, Rehner SA, Aoki T, Robert VARG, Crous PW, Groenewald JZ, Kang S, Geiser DM. 2013. Phylogenetic analyses of *RPB1* and *RPB2* support a middle Cretaceous origin for a clade comprising all agriculturally and medically important fusaria. Fungal Genetics and Biology 52:20–31.

O'Donnell K, Ward TJ, Robert VARG, Crous PW, Geiser DM, Kang S. 2015. DNA sequence-based identification of *Fusarium*: current status and future directions. Phytoparasitica 43:583–595.

Otero-Colina G, Rodríguez-Alvarado G, Fernández-Pavía S, Maymon M. Ploetz RC, Aoki TA, O'Donnell K, Freeman S. 2010. Identification and characterization of a novel etiological agent of mango malformation disease in Mexico, *Fusarium mexicanum* sp. nov. Phytopathology 100:1176–1184.

Pfunder M, Roy BA. 2000. Pollinator-mediated interactions between a pathogenic fungus, *Uromyces pisi* (Pucciniaceae), and its host plant, *Euphorbia cyparissias* (Euphorbiaceae). American Journal of Botany 87:48–55.

Raguso RA, Roy BA. 1998. 'Floral' scent production by *Puccinia* rust fungi that mimic flowers. Molecular Ecology 7:1127–1136.

Rehner SA, Buckley E. 2005. A *Beauveria* phylogeny inferred from nuclear ITS and EF1-α sequences: evidence for cryptic diversification and links to *Cordyceps* teleomorphs. Mycologia 97:84–98.

Roy BA. 1993. Floral mimicry by a plant pathogen. Nature 362:56–58.

Santiago R, Reid LM, Zhu X, Butrón A, Malvar RA. 2010. *Gibberella* stalk rot (*Fusarium graminearum*) resistance of maize inbreds and their F_1 hybrids and their potential for use in resistance breeding programs. Plant Breeding 129:454–456.

Seifert K, Morgan-Jones G, Gams W, Kendrick B. 2011. The genera of hyphomycetes. CBS Biodiversity Series 9. Utrecht, The Netherlands: CBS-KNAW Biodiversity Centre. 997 p.

Srivastava SK, Huang X, Brar HK, Fakhoury A, Bluhm BH, Bhattacharyya MK. 2014. The genome sequence of the fungal pathogen *Fusarium virguliforme* that causes sudden death syndrome in soybean. PLoS ONE 9:e81832.

Steenkamp ET, Wingfield BD, Coutinho TA, Zeller KA, Wingfield MJ, Marasas WFO, Leslie JF. 2000. PCR-based identification of *MAT-1* and *MAT-2* in the *Gibberella fujikuroi* species complex. Applied and Environmental Microbiology 66:4378–4382.

Summerell BA. 2019. Resolving *Fusarium*: current status of the genus. Annual Review of Phytopathology 57:323–339.

Taylor JW, Jacobson DJ, Kroken S, Kasuga T, Geiser DM, Hibbett DS, Fisher MC. 2000. Phylogenetic species recognition and species concepts in fungi. Fungal Genetics and Biology 31:21–32.

Tsavkelova E, Oeser B, Oren-Young L, Israeli M, Sasson Y, Tudzynski B, Sharon A. 2012. Identification and functional characterization of indole-3-acetamide-mediated IAA biosynthesis in plant-associated *Fusarium* species. Fungal Genetics and Biology 49:48–57.

Vrabka J, Niehaus E-M, Münsterkötter M, Proctor RH, Brown DW, Novák O, Pěnčik A, Tarkowská D, Hromadová K, Hradilová M, Oklešt'ková J, Oren-Young L, Idan Y, Sharon A, Maymon M, Elazar M, Freeman S, Güldener U, Tudzynski B, Galuszka P, Bergougnoux V. 2019. Production and role of hormones during interaction of *Fusarium* species with maize (*Zea mays* L.) seedlings. Frontiers in Plant Science 9:1936, doi:10.3389/fpls.2018.01936

White TJ, Bruns T, Lee S, Taylor JW. 1990. Amplification and direct sequencing of fungal ribosomal genes for phylogenetics. In: Innis MA, Gelfand DH, Sninsky JJ, White TJ, eds. PCR protocols: a guide to methods and applications. San Diego, California: Academic Press. p. 315–322.

Zeller KA, Summerell BA, Bullock S, Leslie JF. 2003. *Gibberella konza* (*Fusarium konzum*) sp. nov. from prairie grasses, a new species in the *Gibberella fujikuroi* species complex. Mycologia 95:943–954.

Zhou X, O'Donnell K, Kim H-S, Proctor RH, Doehring G, Cao Z-M. 2018. Heterothallic sexual reproduction in three canker-inducing tree pathogens within the *Fusarium torreyae* species complex. Mycologia 110:710–725.